AD-E200476

AFWL-TR-78-240

AFWL-TR-
78-240

ADA085583

THE BEHAVIOR OF THIN DIELECTRICS UNDER ELECTRON IRRADIATION

B. Goplen, et al.

Science Applications, Inc.
1200 Prospect Street
La Jolla, CA 92037

March 1980

Final Report

LEVEL

Approved for public release; distribution unlimited.

DTIC
SELECTE
JUN 1 8 1980

C

AIR FORCE WEAPONS LABORATORY
Air Force Systems Command
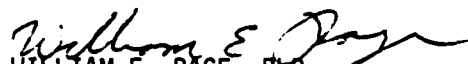Kirtland Air Force Base, NM 87117

80 4 10 030

DDC FILE COPY

This final report was prepared by Science Applications, Inc., La Jolla, California, under Contract F29601-77-C-0021, AFOSR 2311Y101 with the Air Force Weapons Laboratory, Kirtland Air Force Base, New Mexico. Dr. William E. Page (NTMT) was the Laboratory Project Officer-in-Charge.

When US Government drawings, specifications, or other data are used for any purpose other than a definitely related Government procurement operation, the Government thereby incurs no responsibility nor any obligation whatsoever, and the fact that the Government may have formulated, furnished, or in any way supplied the said drawings, specifications, or other data, is not to be regarded by implication or otherwise, as in any manner licensing the holder or any other person or corporation, or conveying any rights or permission to manufacture, use, or sell any patented invention that may in any way be related thereto.

This report has been authored by a contractor of the United States Government. The United States Government retains a nonexclusive, royalty-free license to publish or reproduce the material contained herein, or allow others to do so, for the United States Government purposes.
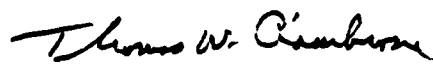
This report has been reviewed by the Public Affairs Office and is releasable to the National Technical Information Service (NTIS). At NTIS, it will be available to the general public, including foreign nations.

This technical report has been reviewed and is approved for publication.

WILLIAM E. PAGE, PhD
Project Officer

FOR THE DIRECTOR

J. PHILIP CASTILLO, PhD
Chief, Technology Branch

THOMAS W. CIAMBRONE
Colonel, USAF
Chief, Applied Physics Division

REPORT DOCUMENTATION PAGE		READ INSTRUCTIONS BEFORE COMPLETING FORM
1. REPORT NUMBER AFWL-TR-78-240	2. GOVT ACCESSION NO. AD-A085 583	3. RECIPIENT'S CATALOG NUMBER
4. TITLE (and Subtitle) THE BEHAVIOR OF THIN DIELECTRICS UNDER ELECTRON IRRADIATION		5. TYPE OF REPORT & PERIOD COVERED Final Report
		6. PERFORMING ORG. REPORT NUMBER
7. AUTHOR(s) B. Goplen W. A. Seidler* W. R. Thomas A. Greenwald*		8. CONTRACT OR GRANT NUMBER(s) F29601-77-C-0021**
9. PERFORMING ORGANIZATION NAME AND ADDRESS Science Applications, Inc. 1200 Prospect Street La Jolla, CA 92037		10. PROGRAM ELEMENT, PROJECT, TASK AREA & WORK UNIT NUMBERS 61102F/WDNE0714
11. CONTROLLING OFFICE NAME AND ADDRESS Air Force Weapons Laboratory (NTMT) Kirtland Air Force Base, NM 87117		12. REPORT DATE March 1980
		13. NUMBER OF PAGES 44
14. MONITORING AGENCY NAME & ADDRESS(if different from Controlling Office)		15. SECURITY CLASS. (of this report) Unclassified
		15a. DECLASSIFICATION/DOWNGRADING SCHEDULE

16. DISTRIBUTION STATEMENT (of this Report)

Approved for public release; distribution unlimited.

17. DISTRIBUTION ST. 'ENT (of '· · abstract entered in Block 20, if different from Report)

18. SUPPLEMENTARY TES

*Subcontractor, Spire Corporation, Bedford, MA 01730
**Research was supported by AFOSR 2311Y101.   61102F

19. KEY WORDS (Continue on reverse side if necessary and identify by block number)

Dielectrics
Electron Irradiation
Test Methods
Electromagnetic Pulses

20. ABSTRACT (Continue on reverse side if necessary and identify by block number)

An experimental and analytical investigation has been made of the anomalous behavior of an electron beam in the presence of dielectrics. The configuration considered is an internal cavity, with electron beam anode on one end and a Faraday cup on the other. Experiments were performed for an empty cavity (vacuum case) and also with a thin dielectric sheet immediately adjacent to the cylinder wall. Variations include the type of dielectric and the use of a screen at the vacuum-dielectric interface. The experimental evidence is that,

while transmitted current is very low for the empty cavity, the presence of dielectric causes considerable enhancement in transmission.

This experiment was modelled analytically using MAD2, a 2-D SGEMP code, to determine the cause of this behavior. Low transmission for the vacuum case is shown due initially to beam spreading (coulomb repulsion) and at later stages to extreme space-charge limiting. It is also demonstrated that enhancement is not due to the electromagnetic effect of dielectric charging. Rather, creation of a plasma at the dielectric surface is hypothesized as the probable effect, with plasma electrons providing breakdown of the space-charge barrier, and positive ions providing charge neutralization and pinching of the beam. Detailed calculations using a simple plasma model give good agreement with experimental data. However, no physical mechanism for the plasma creation process is suggested.

TABLE OF CONTENTS

LIST OF FIGURES

SECTION I

INTRODUCTION

1. BACKGROUND

A series of cavity IEMP experiments reported by Little in 1974 (reference 1) indicated anomalous behavior due to the presence of thin dielectrics within the cavity. The basic observation was that a marked enhancement in transmitted current occurred if a dielectric sheet was present in the chamber under vacuum. (The original experiments will be discussed in detail shortly.) This enhancement effect tended to be relatively independent of dielectric shape and orientation in the chamber. Similarities to current enhancement due to pressure (air) effects were noted. Several possible mechanisms were suggested which might cause the enhancement, including dielectric charging, electrical breakdown through the dielectric, surface flashover, and ion production. However, the responsible mechanism was not identified.

The behavior of dielectrics exposed to photon, charged particle, or electromagnetic radiation is a subject of concern in many fields. For example, dielectrics constitute one of the principal surface materials used in satellites. As such, their behavior is of concern in SGEMP (system-generated electromagnetic pulse), which involves the electrical response of the satellite structure to X rays from a nuclear burst. Incident X rays cause photoemission from the structure itself, thus giving rise to an electromagnetic pulse. Driven electric fields and surface currents on conductors may lead to large charge imbalance, and very strong normal and transverse

---

[1] R. G. Little, R. Lowell, and J. R. Uglum, "Cavity Current Enhancement by Dielectrics," IEEE Trans. on Nuclear Science, V. NS-21, Dec. 1974, p. 249.

fields in adjoining dielectrics. The physical behavior of the dielectric under such conditions may affect system S/V (survivability/vulnerability).

Space-craft charging is another possible area of concern. This phenomenon is believed to involve electrical discharge resulting from the interaction at the satellite structure with the ambient plasma. The resulting discharge process may be sufficiently severe to disable the spacecraft; a number of losses have been attributed to the space-craft charging process. Once again, it is likely that the physical properties of the dielectric play a key role.

This report presents the results from an investigation of dielectric behavior under electron irradiation. The main intent was the identification of those physical processes which so radically affected electron beam behavior in the cavity IEMP experiments. The present investigation proceeded in two concurrent phases. First, based upon preliminary analyses, a series of experiments were designed and carried out at the SPIRE Corporation in Bedford, Massachusetts, using the SPI 6000 electron gun. Variations in these experiments were designed specifically to discriminate against certain of the possible physical mechanisms. Second, in the analysis phase, a series of very detailed calculations were carried out by Science Applications, Inc. in Albuquerque, New Mexico, using the two-dimensional SGEMP code, MAD2. These calculations were designed to accurately simulate the experimental configuration. Theoretical models of the relevant physical processes were contrived and tested in an attempt to explain experimental results.

The experimental phase of this investigation is described in Section II of this report. The analytical approach and physical models are discussed in Section III. Section IV compares experimental and calculated results; conclusions and implications are summarized in Section V.

The remainder of this section provides an overview of the previous cavity experiments, possible current enhancement mechanisms, and a more detailed description of the technical approach taken in the present investigation.

2. PREVIOUS EXPERIMENTAL DATA

Results of the original dielectric experiments are reported in detail in reference 2. The basic geometry involved a cylindrical cavity with metallic walls, which could be evacuated to a pressure of 10^{-4} torr. At one end of the cylinder, a pulsed electron beam accelerator was used to inject electrons into the cavity. The accelerator anode consisted of a fine wire mesh imbedded in mylar; this also served as one end of the cylinder. At the other end of the cylinder, a Faraday cup was used to collect charge transmitted through the cavity.

Properties of the injected electron beam would indicate a substantial degree of space-charge limiting. The beam current approximated a Gaussian shape in time, with peak of about 11 kA and FWHM of about 10 sh. The beam was also monoenergetic at any given time, initially constant at about 100 keV, then decreasing after 6 sh linearly to vanish at the end of the pulse. Variation with polar angle at the anode surface was very slight.

---

[2]J. R. Uglum, R. G. Little, and S. H. Face, "Electron Beam IEMP Simulation Development," Defense Nuclear Agency Report DNA-3986F, August 1975.

The series of tests in the original experiment involved measuring Faraday current for several configurations, including good vacuum, and various air pressure levels. Several tests were also made with dielectric material inside the cavity. For the vacuum case, very little of the injected current was transmitted through the cavity to the cup. Introduction of air into the cavity provided the expected enhancement in transmitted current associated with charge neutralization. Surprisingly, the presence of dielectrics in the cavity (under good vacuum) also resulted in substantial enhancement, producing results similar to those due to pressure (air) effects.

These results tended to be relatively independent of the dielectric geometry. Dielectric material was placed within the cavity in three configurations:

    (a)   a sheet of material positioned perpendicular to the beam at the center of the cavity

    (b)   a sheet along the side wall

    (c)   a cylindrical rod mounted coaxially along the cavity center line.

In each case the transmitted current was significantly enhanced when compared to the vacuum (no dielectric) result.

Results from configuration (a) showed that the transmitted current decreased rapidly as the dielectric thickness approached an electron ($\sim$100 keV)

range. The substitution of an aluminum plate for the dielectric produced less enhancement indicating that the dielectric was not acting simply as a ground plane. Using configuration (b), transmitted current was measured as a function of cavity aspect ratio, injected current pulse width, dielectric thickness, etc. To investigate the possibility of space charge neutralization of the beam by ions, a special ion detector was attached to the cavity back wall. Ions were detected, and the quantities appeared to be much greater than would be expected from ionization of the ambient chamber gas. In addition, a photograph of a lucite dielectric under irradiation in the cavity showed significant amounts of light, possibly produced by a type of dielectric breakdown called surface flashover. A further observation of significance involved the distribution of charge collected on the Faraday cup. For all cases, the collected charge was concentrated near the center of the cup, thus suggesting a pinching effect.

In configuration (c) the beam was observed to focus itself on the dielectric rod about 2-3 cm from the injection plane. In addition, the transmitted current time history was found to be similar to that caused by ambient gas.

3.   POSSIBLE CURRENT ENHANCEMENT MECHANISMS

In attempts to explain the current enhancement phenomonen, several processes have been suggested. The main ones of interest are described briefly below. The objective of the present investigation was to isolate those processes responsible for the dielectric effect.

In the coaxial rod and side wall configurations, it would be possible for electrons to bury themselves within the dielectric. If the dielectric remains a good insulator, the charge will be essentially immobile. It is possible that this trapped charge could focus the radially diverging beam in the side wall configuration. However, negative charge on the coaxial rod tends to cause a greater divergence of the beam, and thus less transmitted current.

If the normal electric fields through a dielectric become high enough, say 10^7 V/m, the dielectric will become conducting and thus allow charge flow. Such a breakdown could release trapped charge in the dielectric, the freed electrons could then flow back toward the emitting surface and thus reduce the normal fields in this region (these fields tend to pull injected electrons into the emitting surface).

One should also consider the production of charge at the dielectric surface. The presence of positive ions in the cavity would tend to neutralize (depending upon their density) the electrostatic repulsion of electrons in the beam. The beam would be pinched by its own magnetic field, and thus be concentrated near the cavity axis. Positive ions could conceivably be produced by several different mechanisms. For example, electrons striking the dielectric might release trapped gas, resulting in gas focusing (magnetic pinch). Thermal heating of the

8

dielectric would be expected to produce low energy ions if enough energy per unit volume was deposited by the impacting electrons. These ions could conceivably be drawn into the cavity by the existing electric fields. Surface flashover, a type of dielectric breakdown, could also produce ions. If the tangential electric fields exceed a threshold value (typically 10^6 to 10^7 V/m), the surface in that region becomes highly conducting. Associated with this breakdown is a burst of a neutral plasma. The positive ions in this plasma could then cause a magnetic pinch of the electron beam. In addition, the plasma electrons could either (1) flow toward the Faraday cup and add to the transmitted current or (2) flow back toward the emitting surface (anode) and reduce the normal electric fields. Secondary electron production (resulting from interaction of energetic beam electrons with the dielectric) represents another potential mechanism for charge creation.

4. TECHNICAL APPROACH

The approach taken in this investigation of the enhancement
phenomenon included both experimental and analytical phases.

The experimental phase was conducted at the SPIRE Corporation
facilities at Bedford, Mass. It involved repeating the original experiment
by Little, but with modifications directed at isolating the current enhance-
ment process. In these experiments, the SPIRE 6000 electron gun was used
to inject a beam into one end of a closed, cylindrical cavity with
dimensions of 15 cm radius and 15 cm length. The primary measurement
consisted of a Faraday cup current obtained at the cylinder end opposite
the beam injection. The basic experiment was performed with perfectly
conducting outer walls. Subsequently, thin layers of dielectric were
inserted adjacent the outer walls of the cylinder. Variations included
the type and thickness of dielectric. In addition, conducting wire meshes
of various sizes were then placed immediately adjacent to the dielectric
surface to modify the nature of the electric fields at the vacuum-dielectric
interface.

In the analytical phase, the experimental configuration described
above was simulated using the two-dimensional SGEMP code MAD2. This work
was performed by Science Applications, Inc. at Albuquerque, New Mexico.
Injected beam characteristics (energy and current vs time) were modelled
from the experimental data. An electromagnetic model of thin dielectrics
(including charging) was developed which is compatible with large grid
spacing. A simple model for ion (and electron) production from the
dielectric surface was also developed. This analytical tool was then used

10

to demonstrate that the experimental enhancement of transmitted current could, indeed, be caused by production of a plasma at the dielectric surface.

SECTION II

EXPERIMENTAL PROGRAM
(Reference 3)

1.   TEST GEOMETRY

The experimental test configuration is illustrated in figure 1. An electron beam was injected into a 30 cm x 15 cm cylindrical cavity. The beam was obtained using the SPI-6000 machine, having the following characteristics:

mean electron energy	- 77 keV ±20%
current	- 10 kA ±10%
beam size	- 30 cm diameter
pulse width	- 100 ns ±20%
rise time	- 50 ns ±10%
beam variation over 730 cm^2	- 20%

Measurements performed for these experiments included:

(1) The injected current measured by a 30 cm diameter aluminum Faraday collector placed 2mm from the anode mesh inside the chamber.

(2) The injected current measured by a calibrated resistor ring between the anode mesh and the surface of the 30 cm aluminum test chamber.

---

[3]W. A. Seidler, "Experimental Determination of Plasma Release from Electron-Irradiated Dielectrics Stressed by Transient Electric Fields," SPIRE Corp Report FR-20065 prepared for SAI under Subcontract SAI-1-101-32-816-03, March 1978.
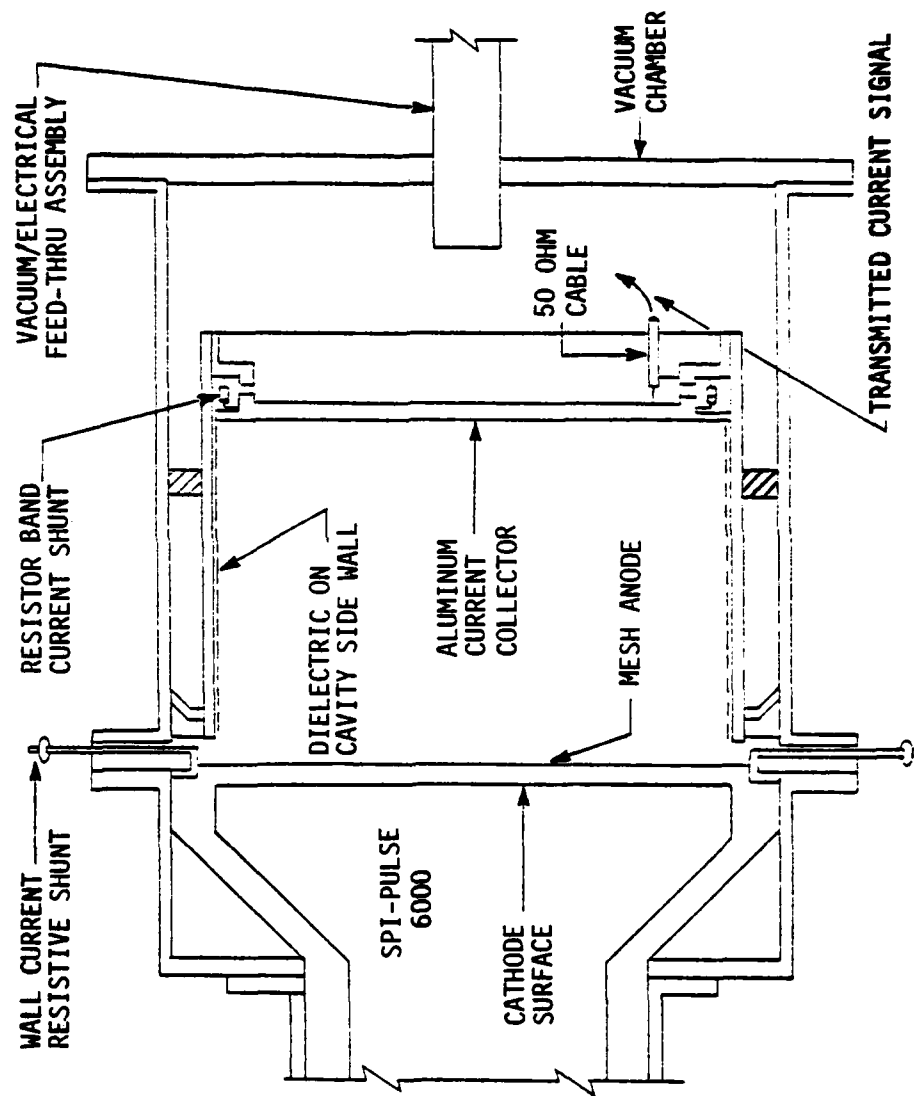
Figure 1

Test Configuration

13

(3) The current transported through the cylinder measured by a 30 cm diameter aluminum Faraday collector.

(4) Ion currents exiting the cylinder measured through a 1 cm axial aperture using a magnetically shielded Faraday collector (not shown).

(5) Velocities of the ion currents exiting the cylinder measured by time of flight techniques (not shown).

(6) The diode voltage measured with a capacitive voltage monitor standard to the SPI-PULSE electron beam machines (not shown).

(7) The diode current measured with a calibrated resistor ring standard to the SPI-PULSE electron beam machines (not shown).

All sensors were calibrated to accuracies better than ±5%. Sensor outputs were recorded by Tektronix 519 oscilloscopes (1 GHz response) or a Tektronix 7844 dual beam oscilloscope (400 MHz response).

2. TEST PLAN

2.1 Injected Beam Parameters.

The general test plan called for initial measurements to be made with the cavity empty (All tests reported here were performed at a pressure of 0.1μ, ±50%). This allowed measurement of electron beam properties by placing the Faraday cup at a distance of 1 cm from the anode mesh. This geometry destroys the space charge well at the anode mesh, and allows the injected beam to propagate to the Faraday cup.

As shown in figure 2, the injected current had a rise time of 40 ns, a pulse width (FWHM) of 94 ns, and a peak output current of 13 kA.

Figure 3 illustrates the electron energy in time as measured from the beginning of the injected current pulse shown in figure 2. The peak electron energy is 108 keV decaying to 20 keV at 150 ns. The electron energy through the rise of the pulse is constant at approximately 100 keV.

This energy spectrum was measured using a 10 channel magnetic spectrometer which has a response time of 100 ps. Each channel of the spectrometer was time synchronized with the Faraday cup current on a dual beam oscilloscope. Time correlation between the current injected into the cavity, figure 2, and the energy spectrum was better than 1 nanosecond. Channel 10, the highest energy channel of the spectrometer, registered no current confirming that no energies were greater than the limits of the spectrometer. The experimental points shown on the plot in figure 3 are overlaid on a solid curve representing the "nominal" electron energy output curve for the SPI-6000.

2.2 Dielectric Tests.

With the Faraday cup in its normal position (15 cm), the beam transmission properties for the evacuated (empty) cavity were determined. Subsequently, tests were initiated using thin sheets of dielectric immediately adjacent to the cylindrical wall, as illustrated in figure 1.
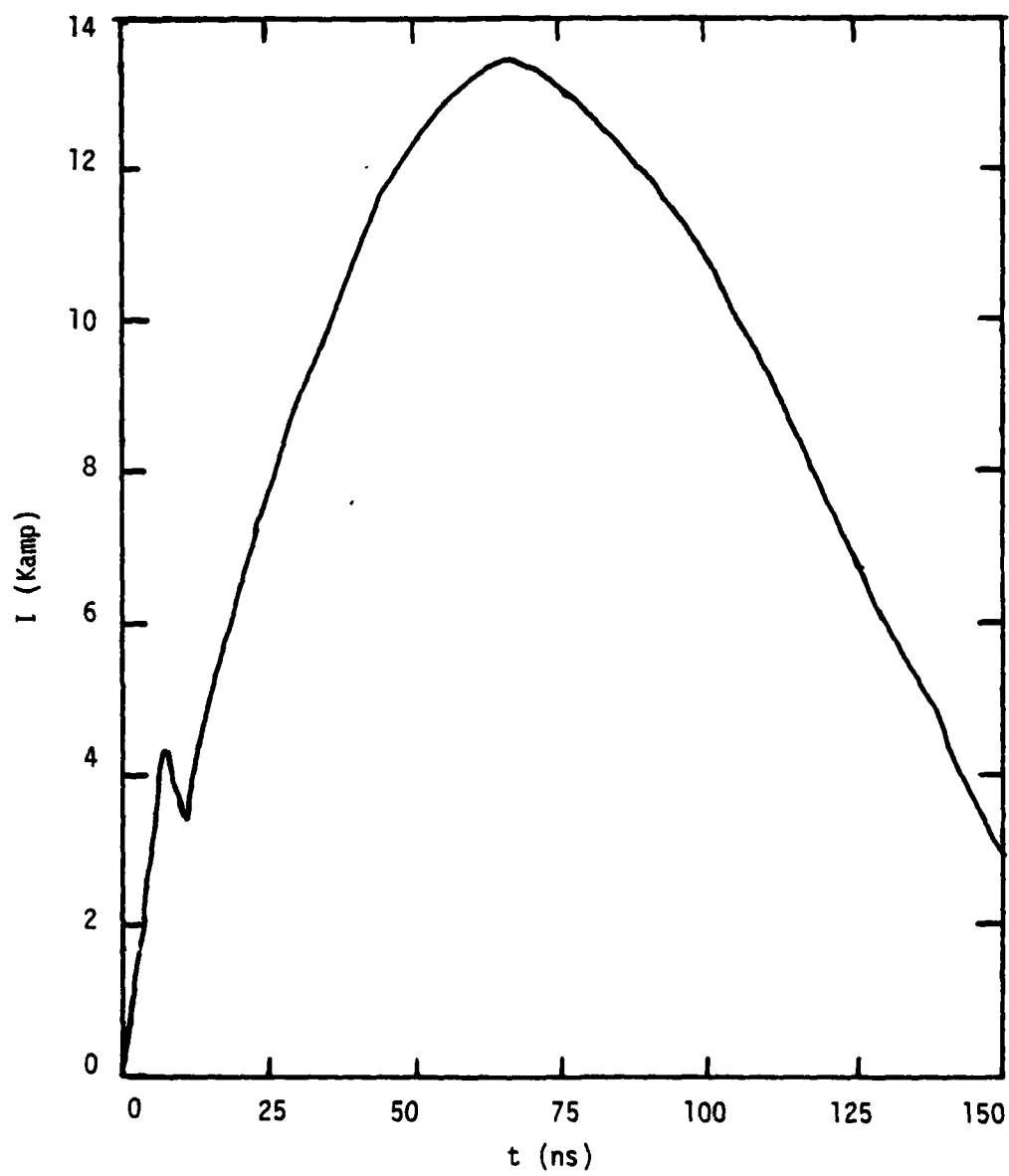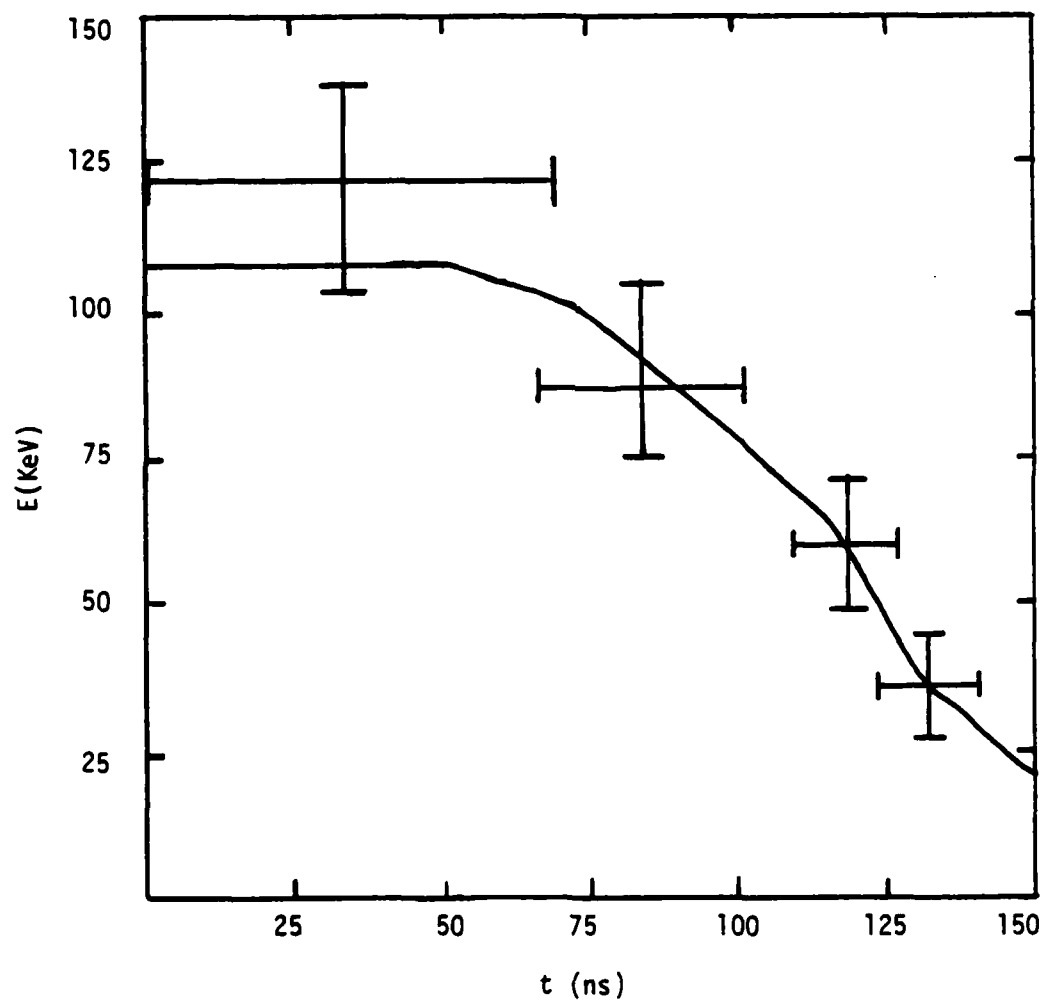
Figure 2

Electron Gun Current Versus Time

16

Figure 3

Injected Electron Energy Versus Time

In hopes of observing variation in results with dielectric parameters, a number of dielectric materials were tested. These included: polyethylene, polystryrene, nylon, Mylar, polyvinyl-chloride, Teflon, Lucite, and silicon rubber. The parameters varied as to dielectric breakdown strength, flashover strength, and thermal breakdown. Table 1 summarizes the electrical properties of the materials irradiated.

In addition to the material variations, a series of tests were also performed in which a metallic screen was placed directly on the dielectric. This was done to change the nature of the electric field distribution near the dielectric surface. Three different metal screens were used, one with coursely meshed long-itudinal strips, one with coarsely meshed circumferential strips, and one with a very fine mesh, interwoven, screen.

3. EXPERIMENTAL RESULTS

The main experimental results of interest are recorded in the Faraday cup measurements illustrated in figures 4 through 7. These results represent current transmitted through the cavity. Figure 4 presents results for the empty cavity (no dielectric) as well as four different dielectrics (Mylar, PTFE (Teflon), polyethylene, and polystyrene). Similar results in figure 5 include the empty cavity (repeated from figure 4) and another four dielectrics (Lucite, PVC, silicon rubber, and nylon).

TABLE 1.

Electrical Properties of Dielectric Material Tested

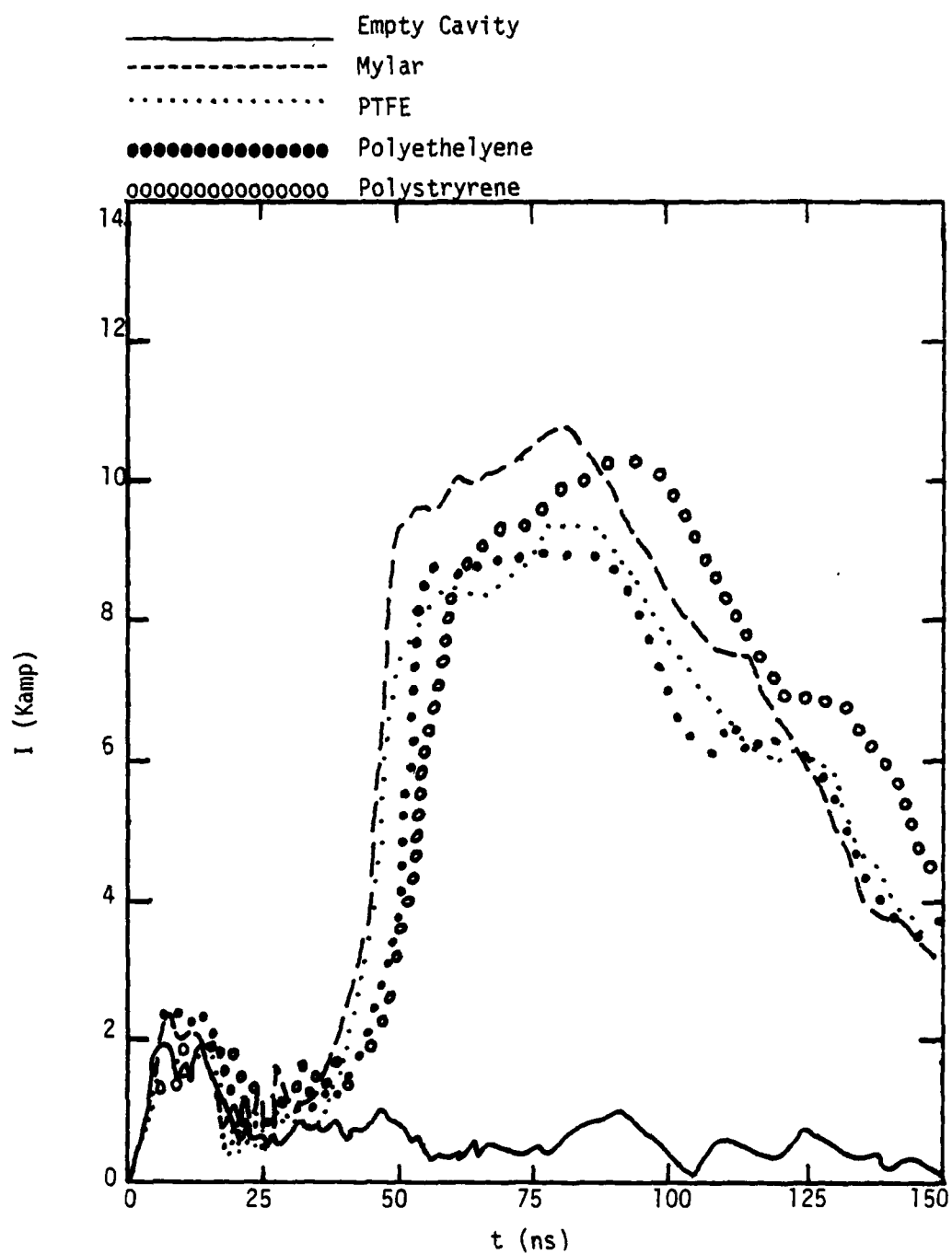| Material	Density (gm/cm³)	Intrinsic Strength 60 Hz (mV/cm)	Dose to Produce Change in Prop. (Megrad)	Heat Distortion Temperature °C	Melt Temperature °C	Dielectric Strength VPM 1/8"	Mils Dielectric Strength VPM	Flashover Strength kV/cm
Polyethylene	0.92	9.0	20.	35-50°	80°	400-500	2500-4700	140-180
Polystyrene	1.04-1.13	4.9, 7.1	800	50-75°	253°	500-700	-	160-200
Nylon	-	6.8, 6.6	-	65-150°	253°	300-400	1500-1700	60-110
Mylar	1.38	5.7	20	230-240°	250°	-	7000-10,000	-
PVC	1.40	4.5	9.0	60-80°	-	450-1300 (rigid) 250-800 (plasticized)	425-1300 250-1000	-
PTFE	-	9.0	0.02	130-135°	330°	400-500	3000-4000	-
Lucite	1.18	9.8	0.8	-	115-180°	800	-	160-200
Silicon Rubber								50

Figure 4

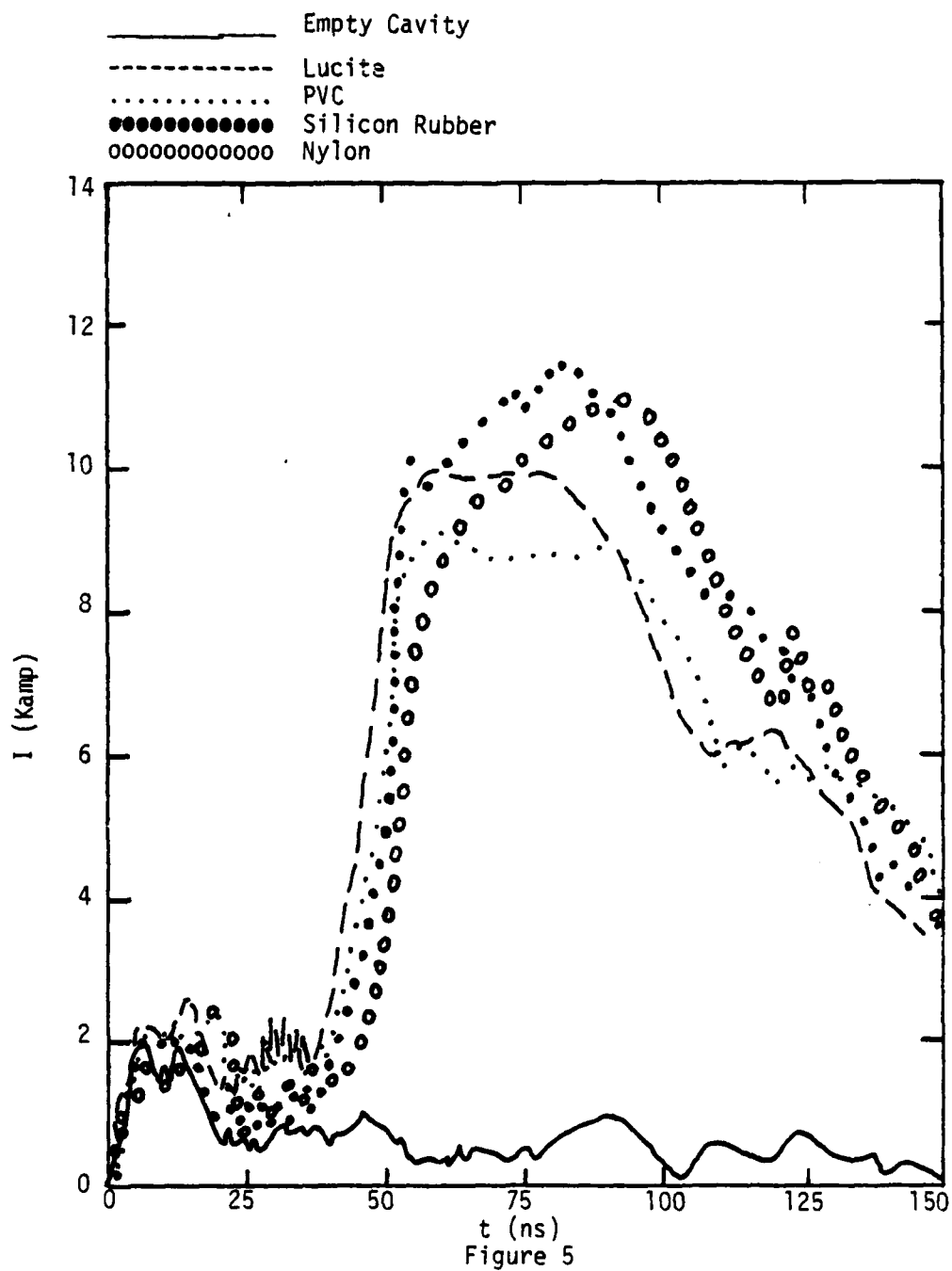Faraday Cup Currents With An Empty Cavity
And Dielectric Liners

Figure 5

Faraday Cup Currents With An Empty Cavity
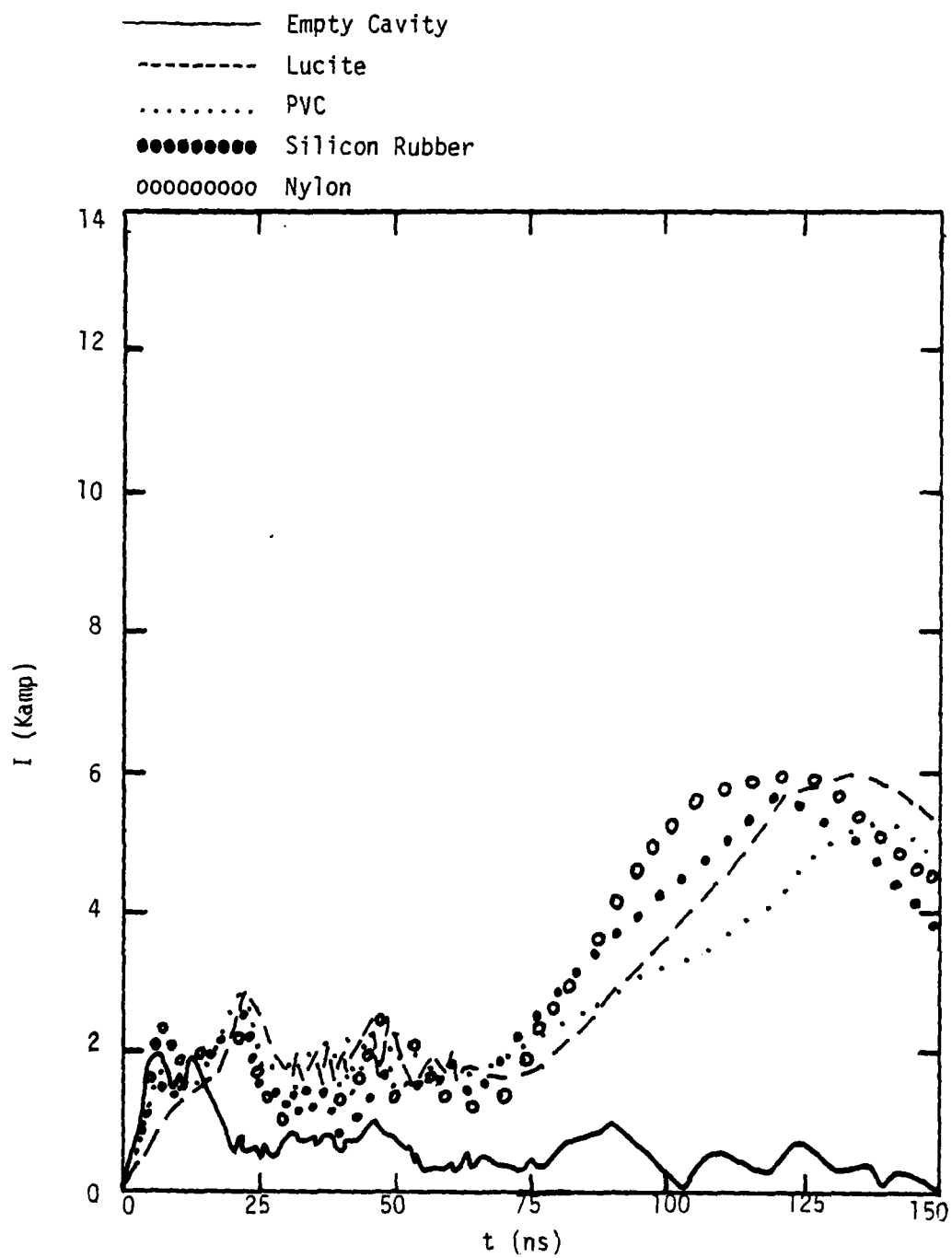And Dielectric Liners

21

Figure 6
Faraday Cup Currents With Dielectrics Covered
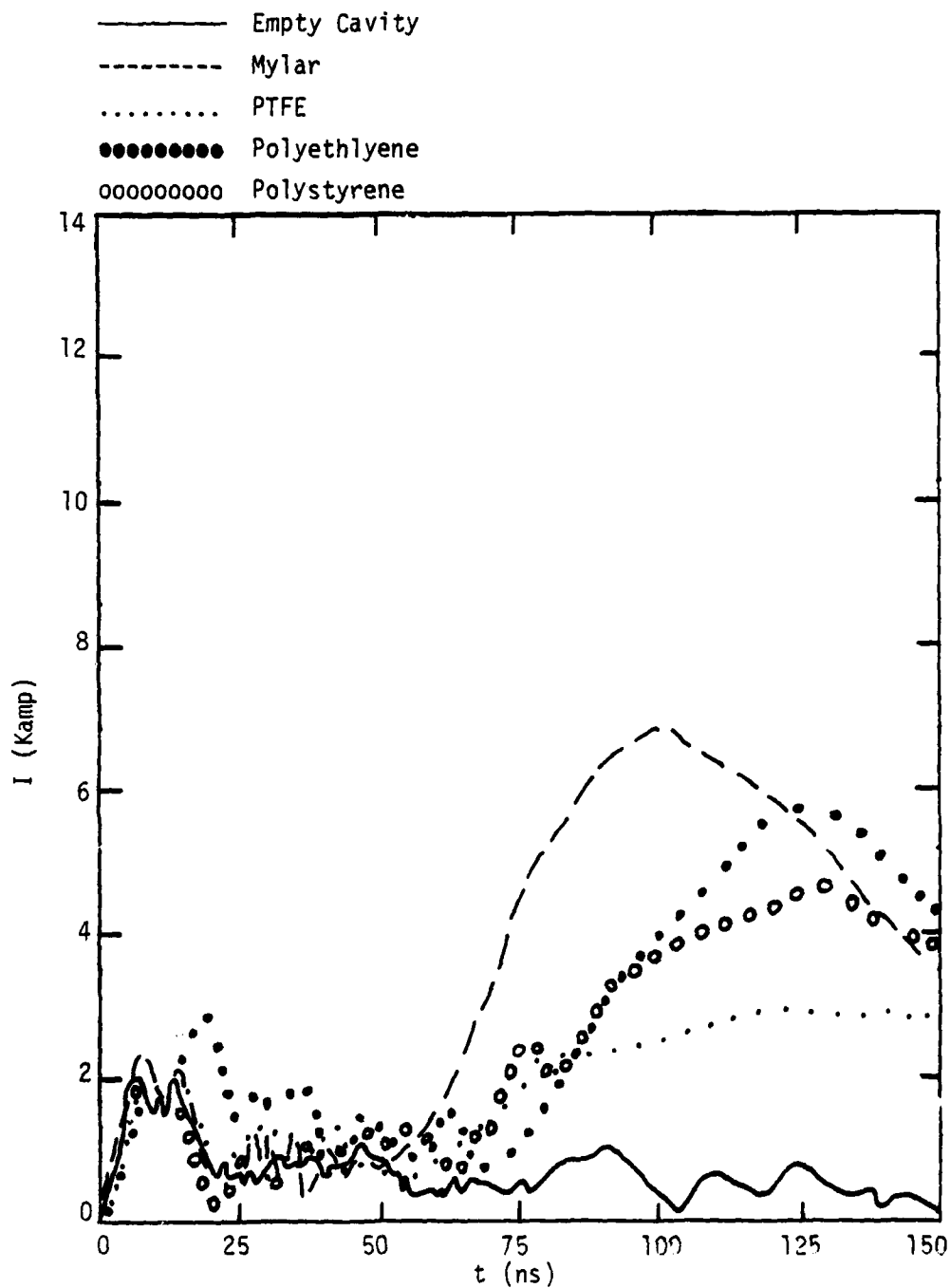By a Grounded Metallic Screen

Figure 7

Faraday Cup Currents With Dielectrics Covered
By a Grounded Metallic Screen

23

Figures 4 and 5 clearly illustrate the enhancement
phenomenon. That is, without dielectric present, the beam pro-
perties in the cavity substantially reduce the transmission of
injected current. For an initial period of about 2 shakes, the
Faraday cup current closely tracks the injected beam current
(see figure 2). At this time, the beam properties change
drastically, and transmission is substantially diminished.

This limited transport feature abruptly changed with
the addition of a dielectric liner. In all cases tested, the
dielectric liner produced a sharp increase in the Faraday cup
current about 4.5 shakes after the first electrons arrived. The
rise time was significantly faster than that of the injected
current pulse by about a factor of four. Roughly three-quarters
of the injected beam peak magnitude was recorded at the Faraday
cup; most significantly, no gross effects due to differences in
the dielectric properties were noticed.

Figures 6 through 7 summarize the similar results obtained
with the different dielectrics covered by an aluminum ground screen.
This screen would tend to reduce the transverse components of electric
field at the surface of the dielectric. Results shown in figures
6 through 7 suggest some dependence on the material properties of
the dielectric. Teflon response to within a factor of 3 of
the case of no dielectric in the cavity, while Mylar produces
only a small reduction in amplitude. All Faraday cup currents
exhibited drastic change in the rise time of the transmitted pulse.

24

To determine effects due to mesh size strips of copper tape were placed over the dielectric surface in the axial and the azimuthal directions (in two separate series of tests). The ends of the strips were grounded on the anode side of the cavity. As the spacing of the stripping was decreased from 2.5 cm to 0.5 cm, the current wave form propagated to the Faraday cup changed from a very sharp rising current characteristic of the dielectric with no grounded screen to the slow rising current characteristic of the ground screen. These effects are illustrated for lucite in figures 8 and 9. These figures also indicate that the field does not depend on azimuthal or longitudinal directions. Both cases of stripping gave the same results for the same spacing. The process did not depend on the area covered by the copper tape since the grounded aluminum screen covered less area.
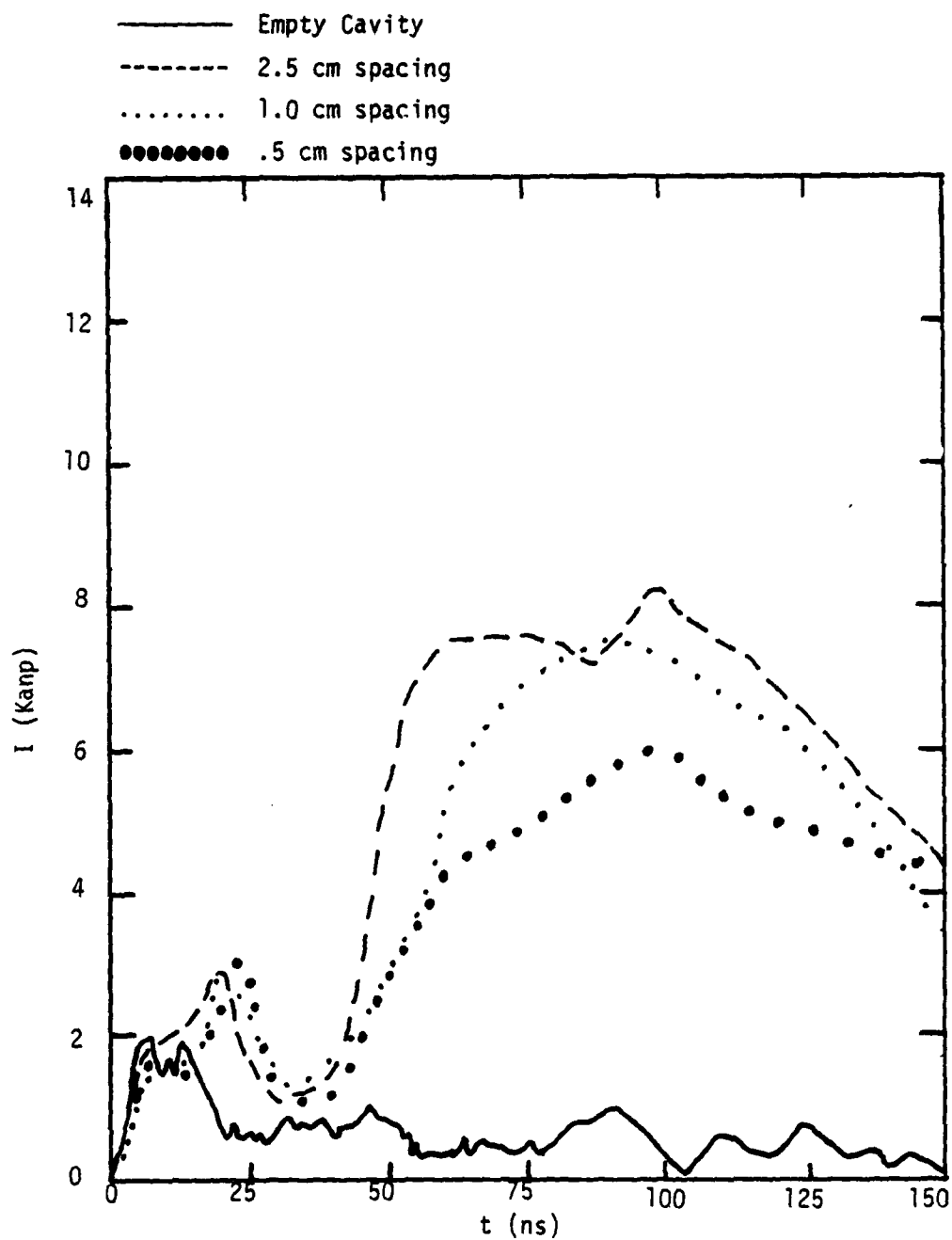
Figure 8
Faraday Cup Currents With Longitudinal
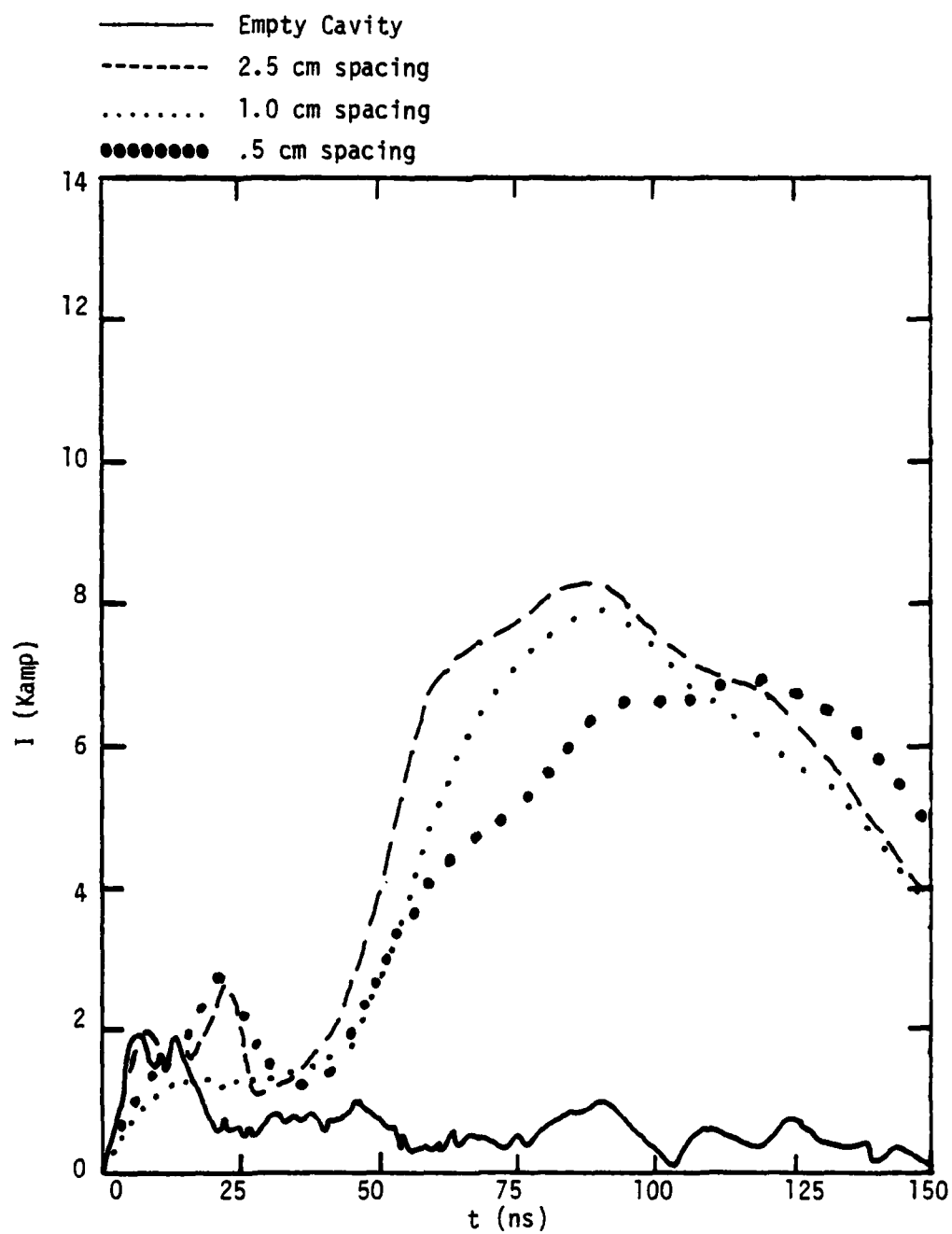Metallic Strips Placed on Lucite

Figure 9

Faraday Cup Currents With Circumferential
Metallic Strips Placed on Lucite

27

SECTION III

ANALYTICAL MODEL DEVELOPMENT

1. METHOD OF CALCULATION

The experimental configuration described in Section II was modelled using the two-dimensional SGEMP code, MAD2. This code is described in detail in reference 4. This section will briefly outline the main features of MAD2, and then describe in detail the modifications made to the code for this simulation.

In its standard form, MAD2 contains a fully dynamic solution of Maxwell's equations, second-order in both spatial coordinates and time. The self-consistent current density sources are obtained by the method of particle pushing. Particle kinematics are fully relativistic and include the full Lorentz force. For these calculations, the inclusion of magnetic forces was, of course, absolutely essential. However, because injected electrons in the experiment were initially axially directed (with little radial spreading), two-dimensional kinematics were adequate. (Ion production at the dielectric surface assumed very small initial velocities.) The overall formalism is time-reversible.

---

[4] B. Goplen, R. E. Clark, and B. Fishbine, "MAD2 - A Computer Code for Systems-Generated Electromagnetic Pulse (SGEMP) Calculations in Two Dimensions," Science Applications, Inc. Report SAI-76-505-AQ, also AFWL-TR-77-26, January 1977.

The high current density produced by the SPIRE 6000 electron gun creates a severe case of space-charge limiting. Were it not for replacement currents into the beam injection surface, the analytical problem would not be tractable with this approach. In effect, the replacement current into the injection surface area tends to reduce normal electric fields, thus reducing the severity of the space-charge limiting problem. Even so, the modelling requirements are formidable, and probably represent the most severe test in level of current density yet attempted with the MAD2 code. This was evidenced most dramatically by the sensitivity of calculated results to the detail of model implementation in the code.

2. ELECTROMAGNETIC MODEL OF A THIN DIELECTRIC

2.1 Derivation of the Model

In general, the dielectric layers in the experiment were much thinner than the size of single cell in the electromagnetic grid. For this reason, it was not possible to treat the dielectric in a brute-force manner electromagnetically. Rather, a model was developed which treats the dielectric properties by means of a boundary layer on the larger electromagnetic grid.

Variables essential to the thin dielectric model are defined in figure 10, which illustrates a unit cell adjacent to the dielectric and perfectly conducting surfaces. The variables E_z^-, E_i^-, E_r^+ and E_r^- represent the defined electric fields on the four sides of the unit cell. The superscripts, + or -, are used to designate axial position in the grid. The variable E_i^- also represents the interface field at the vacuum-dielectric junction, while $E_d^\pm$ represent normal fields within the dielectric itself. The field E_c^- on the dielectric-conductor interface must, of course, vanish; it is included only to make clear the necessary integrations involved in the model.
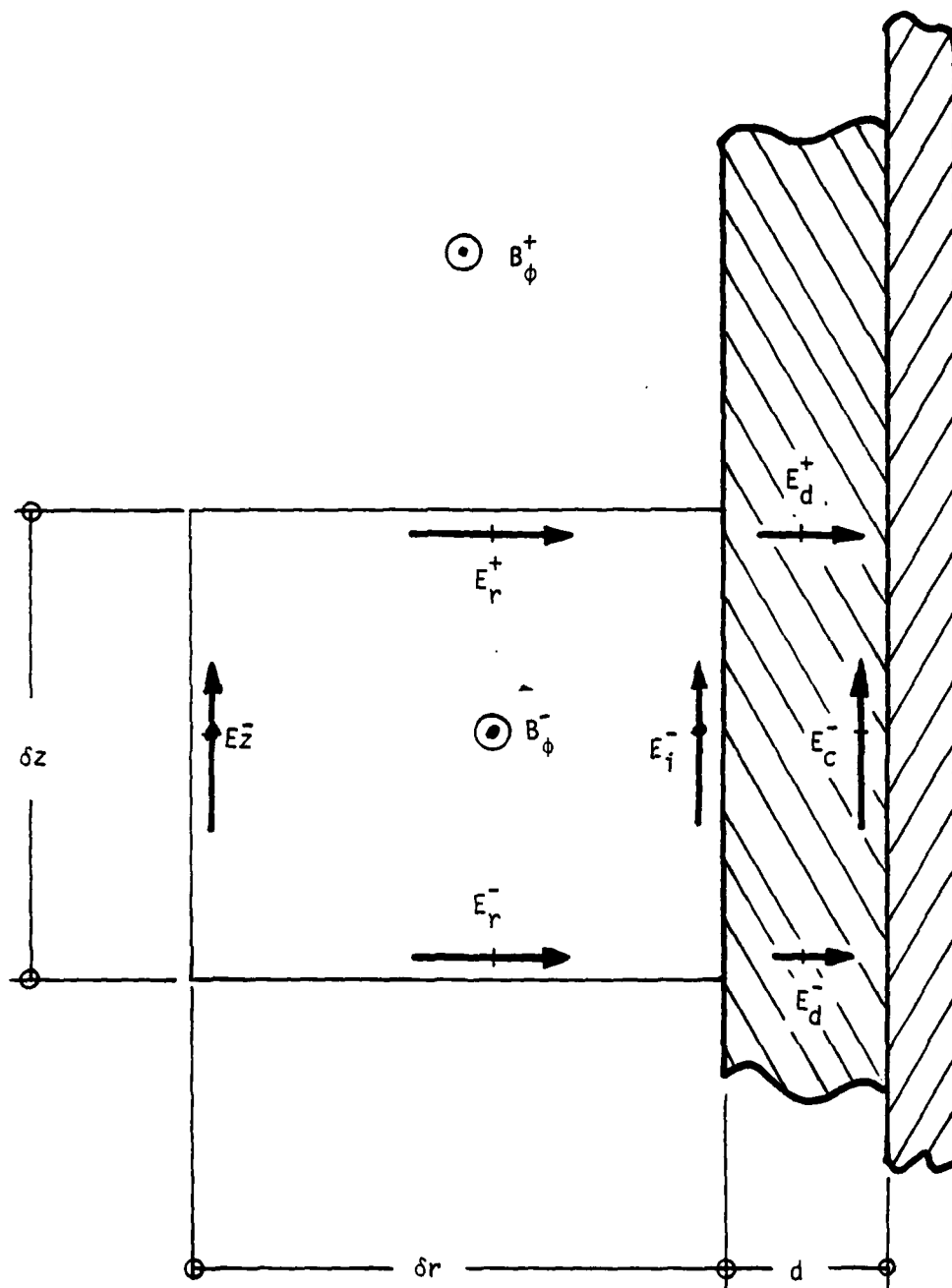
29

Figure 10. Defined Variables in the Thin Dielectric Model.

Maxwell's curl equations, and the constitutive relations between E and D or B and H are (MKS units):

$$\partial_t \bar{D} = \bar{\nabla} \times \bar{H} - \bar{J}$$

$$\partial_t \bar{B} = - \bar{\nabla} \times \bar{E}$$

$$\bar{D} = \kappa \varepsilon_0 \bar{E} \tag{1}$$

$$\bar{B} = \mu_0 \bar{H}$$

where $\bar{D}$ is assumed aligned with $\bar{E}$, and related to it by the dielectric strength, x. The value of x in vacuum is unity; for dielectrics considered here, a typical value is 2.5.

Application of Stokes' theorem to the second curl equation gives

$$\int \overline{dA} \cdot \partial_t \bar{B} = - \oint \bar{E} \cdot \overline{dl} \tag{2}$$

We apply this result separately to two areas: that of the unit cell, and the smaller area to the right within the dielectric. It is next assumed that the magnetic field varies slowly with radius. In this case, the terms, $\partial_t B_\phi$, for the two areas can be equated, and the result solved for the interface field, E_i^-. This result is

$$E_i^- = \frac{d\delta r}{\delta z(d+\delta r)} \left\{ \frac{\delta z}{\delta r} E_z^- + \frac{\delta z}{d} E_c^- + (E_r^+ - E_r^-) - (E_d^+ - E_d^-) \right\} \tag{3}$$

31

As noted before, the conductor field E_c^- vanishes.

Application of Stokes' theorem to the first curl equation yields

$$\int d\bar{A} \cdot \partial_t \kappa \epsilon \bar{E} = \frac{1}{\mu_0} \oint \bar{B} \cdot d\bar{l} - \int d\bar{A} \cdot \bar{J} \qquad (4)$$

Outside the dielectric, application of this result simply gives the standard algorithm result for E_r^+. However, within the dielectric, the result is

$$\delta E_r^+ = \frac{c^2 \delta t}{\kappa \delta z} (B_\phi^+ - B_\phi^-) \qquad (5)$$

Since the dielectric constant differs from unity and the current density varieties. (We assume the electrons to be deposited in a layer much thinner than the dielectric itself.)

The prescription is now complete. Upon completion of the electric field calculation using the standard algorithm, the dielectric fields are calculated from equation (5). Next, the interface fields are calculated using equation (3). These interface fields, which are also defined as fields in the unit cell, thus provide a boundary condition for the magnetic field algorithm on the subsequent time step.

2.2 Validation of the Dielectric Electromagnetic Model

Because the preceding model of the electromagnetic response
of a thin dielectric was vital to current enhancement calculations
(particularly with respect to ion production), it was necessary to
validate this method of calculation. Validation was performed by
a direct comparison of results for the model vs a detailed, brute-
force calculation. These calculations were made for a geometry
similar to the experimental configuration, but used a prescribed
(analytical) source to avoid statistical problems associated with
discrete particle motion. Again, the objective was to demonstrate
the adequacy of the thin dielectric electromagnetic model.

The problem geometry is illustrated in figure 11. This cylinder
matches the internal dimensions of the experimental cavity. The
dielectric sheet adjacent to the outer wall was assumed to be 1/8"
in thickness, with a dielectric constant, κ_1 of 2.5. A prescribed
source of the form

$$\bar{J}(p,t) = \frac{\bar{p} x \tau e^{-\beta \tau}}{p^3} \tag{6}$$

was used, with its origin as shown in figure 11. Representing the
source in this way is intended to approximate a beam produced at
the base of the cavity. The distance and retarded time for this
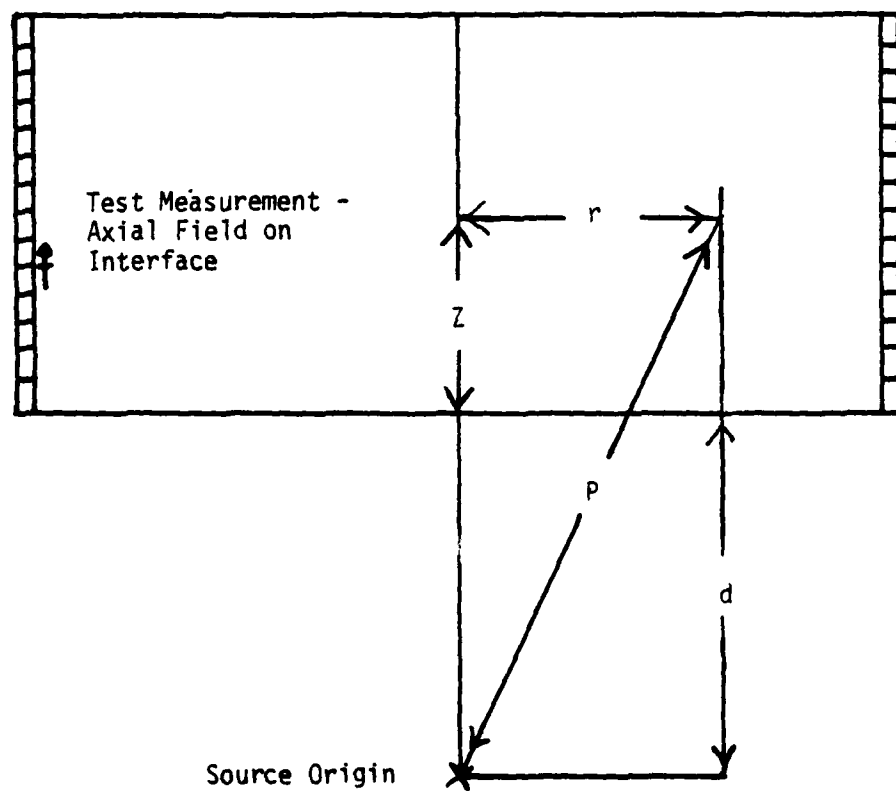source are given by

33

Figure 11

Geometry for the Validation Test

$$p = \left\{ r^2 + (z+d)^2 \right\}^{1/2}$$

$$\tau = t - p/c \qquad\qquad (7)$$

Vector components of the current density in equation (6) were calculated for all defined components of electric field in the grid, except within the dielectric itself. This simulates the deposition of charge at the vacuum-dielectric interface. In this model, charge so deposited is immobile.

In the first calculation, the thin dielectric model was used to simulate the electromagnetic effect of the dielectric sheet. In the vacuum region, a grid spacing of 0.5cm was used in the radial and axial coordinates.

In the brute-force simulation, the dielectric itself was divided into three radial zones of 0.106 cm each. In the vacuum region, non-uniform grid spacing was used to achieve a gradual transition to the fine spacing in the dielectric. In this calculation, a finite-difference solution to Maxwell's equations was obtained everywhere, both in vacuum and in the dielectric. However, in the dielectric region, the current density source was made to vanish, and the dielectric constant $\kappa = 2.5$, was used in Maxwell's equations.

The brute-force approach required a special treatment of boundary conditions at the vacuum-dielectric interface. Consider the possibility of a radial variation in magnetic field. Then the apparent problem is that, although the transverse magnetic field itself must be continuous,

no such constraint exists physically for the radial derivative of this field. This problem was solved by extrapolating magnetic fields from both sides to estimate the value at the interface, and then taking one-sided derivatives. Two separate differential equations were written for the interface field, E_z, reflecting locations slightly to the right (or left) of the interface. These two equations were added together and solved to obtain the interface field. Again, this precaution was taken to allow for a spatial variation in magnetic field near the interface, thus ensuring an adequate brute-force treatment.

Results of the two calculations were characterized by the time histories of the axial electric field located on the vacuum-dielectric interface midway up the cylinder. This field component (illustrated in figure 11) is obviously sensitive to model detail; similar components defined in the corners of the cavity exhibit only slightly greater sensitivity.

The calculated results are presented in figure 12. As can be observed, the two models give reasonable agreement in peak values, and excellent agreement in the overall response throughout the pulse. This measurement was selected for presentation because of the character and sensitivity of this component. Other field components exhibit even

better agreement between the two models. For example, differences in the radial electric fields within the dielectric would be imperceptible in a drawing such as figure 12. This field exhibits a linear rise in time, reflecting charging of the dielectric surface. This field reaches a value of almost 10^8 V/m for this case. The scale is arbitrary, of course, since the problem formulation is linear and the source normalization was arbitrarily chosen. The significant result is the demonstration that the thin dielectric model provides reasonably accurate results. This electromagnetic model was used in all subsequent calculations involving dielectrics.
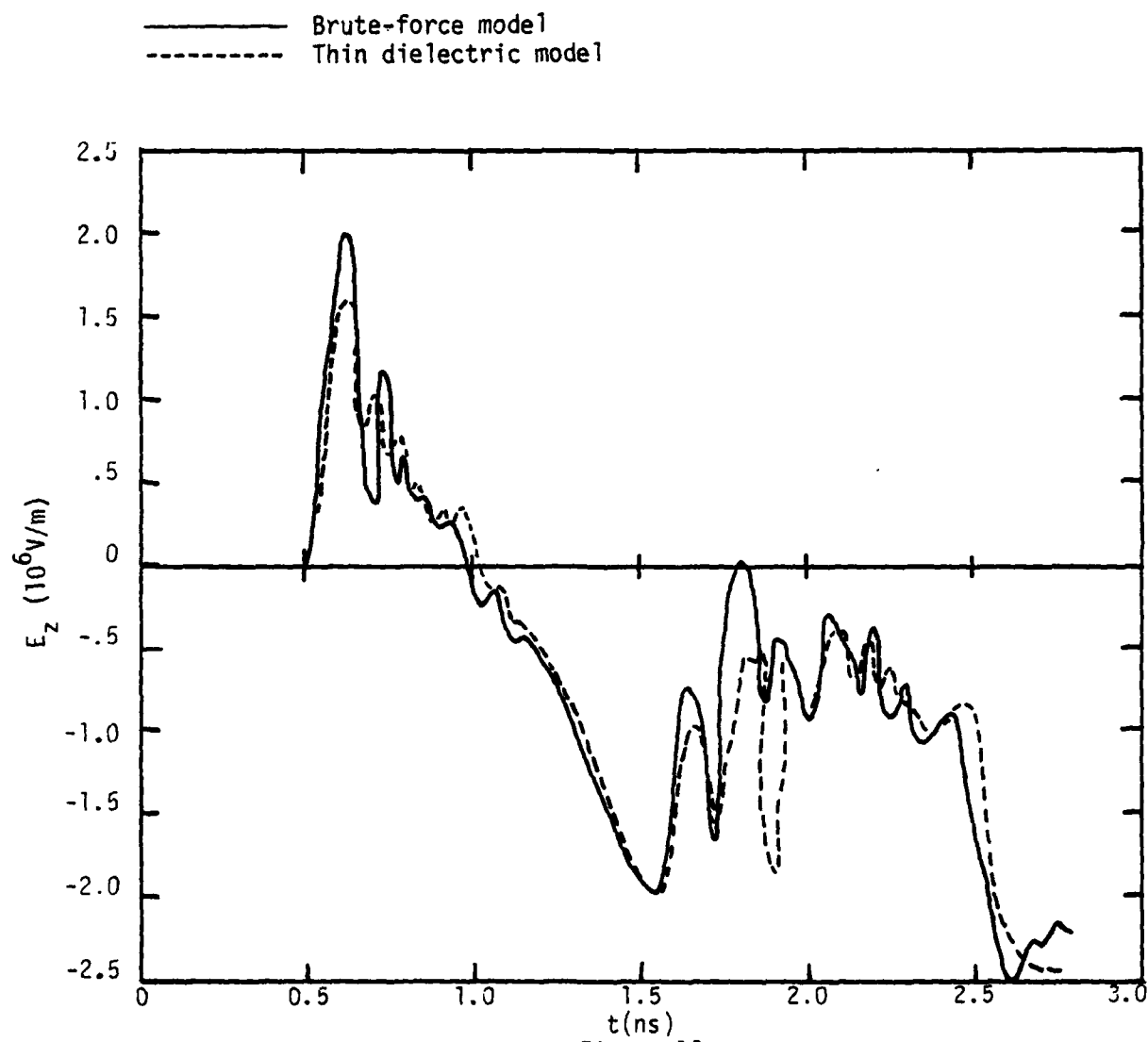
——————— Brute-force model
----------- Thin dielectric model

Figure 12

Calculated Results for the Validation Test

38

SECTION IV

ANALYTICAL RESULTS

1. EMPTY CAVITY AND ELECTROMAGNETIC EFFECTS OF A DIELECTRIC
    LINER

Initially, two separate cases were studied using the MAD2 code.
The first case was a simulation of the empty cavity (no dielectric)
response, while the other included the electromagnetic effects of both
the cavity and dielectric liner. In the latter calculation, the
permittivity was chosen to be equal to 2.5. Figure 13 and 14 show
the Faraday cup currents for these two cases. It can be seen that
the electromagnetic effects of the dielectric actually inhibited the
beam transport to a greater extent than did the empty cavity, although
this result is very sensitive to model detail.

In both of the preceding cases the beam was initially observed
to spread in the radial direction. This was caused by Coulomb repulsion.
At later times ($\gtrsim$ 10 ns) extreme space-charge limiting was present.

2. PLASMA MODEL

It was discovered that the injection of a neutral plasma from the
dielectric could result in a significant Faraday cup current enhancement.
Although the exact mechanism for this plasma formation was unknown, it
was assumed to be associated with the electric field strength along the
vacuum-dielectric interface. Plasma particles (electrons and protons) were
released at regions along the dielectric where the absolute value of the
tangential electric field was greater than 1.5×10^6V/m. The emission rate
for each species was chosen to be 1.0×10^5coul/m^2-sec.

39

The emission was restricted to the first half of the dielectric closest to the electron gun surface so as to prevent large numbers of plasma electrons from reaching the Faraday cup, a situation believed to be unphysical. The particles were injected normal to the surface with very small velocities. Figure 14 shows that a significant current enhancement occurred. The positive ions caused the electron beam to pinch and the plasma electrons moved toward the emitting surface, thereby reducing the high positive fields. Experiments performed with the metal screen and metal strips were simulated in the calculations by using a higher threshold electric field. This had the effect of delaying the plasma release in time. Figure 14 shows the good agreement between the analytical and experimental results for the screened PVC. The threshold electric field used was 4×10^6 V/m.
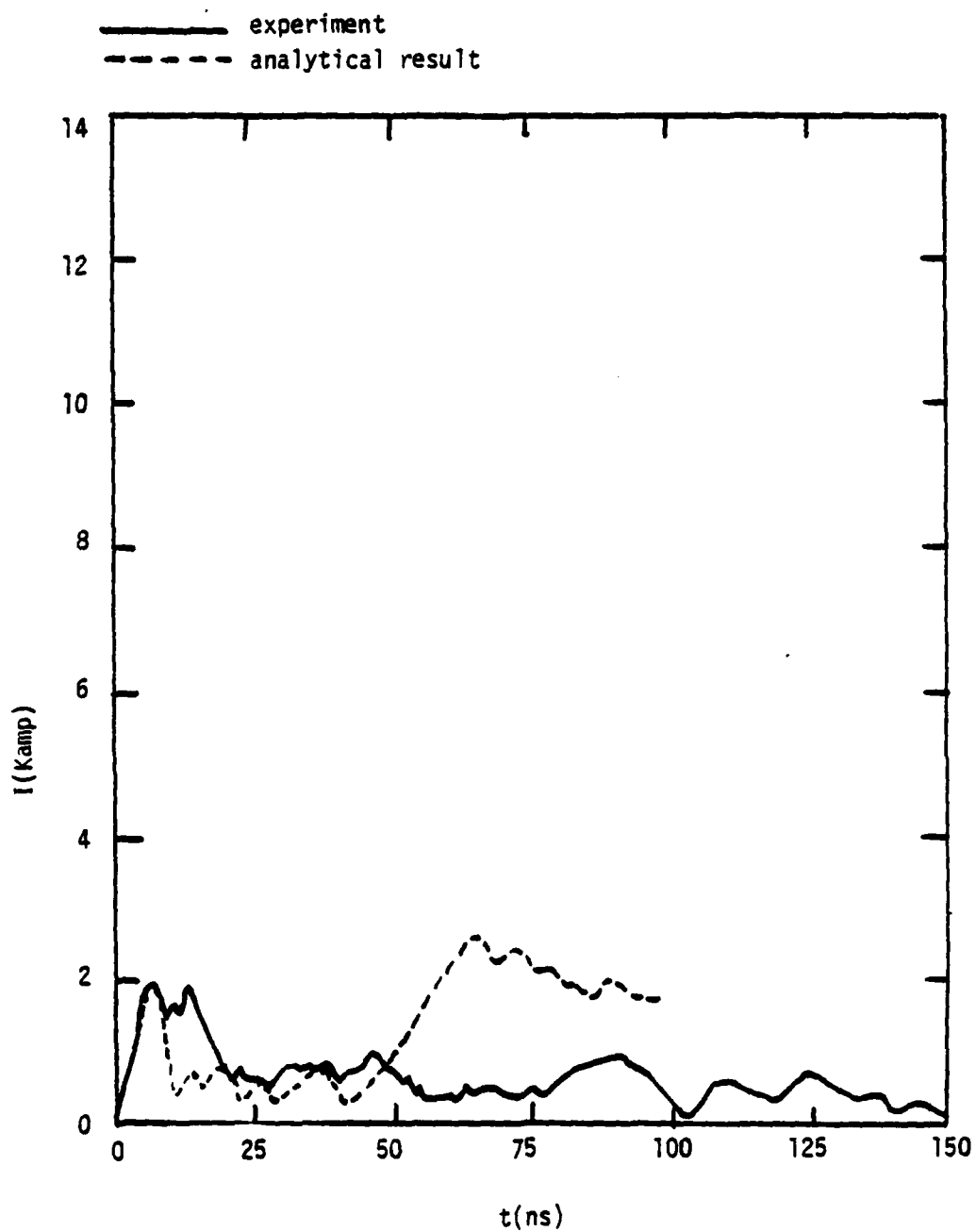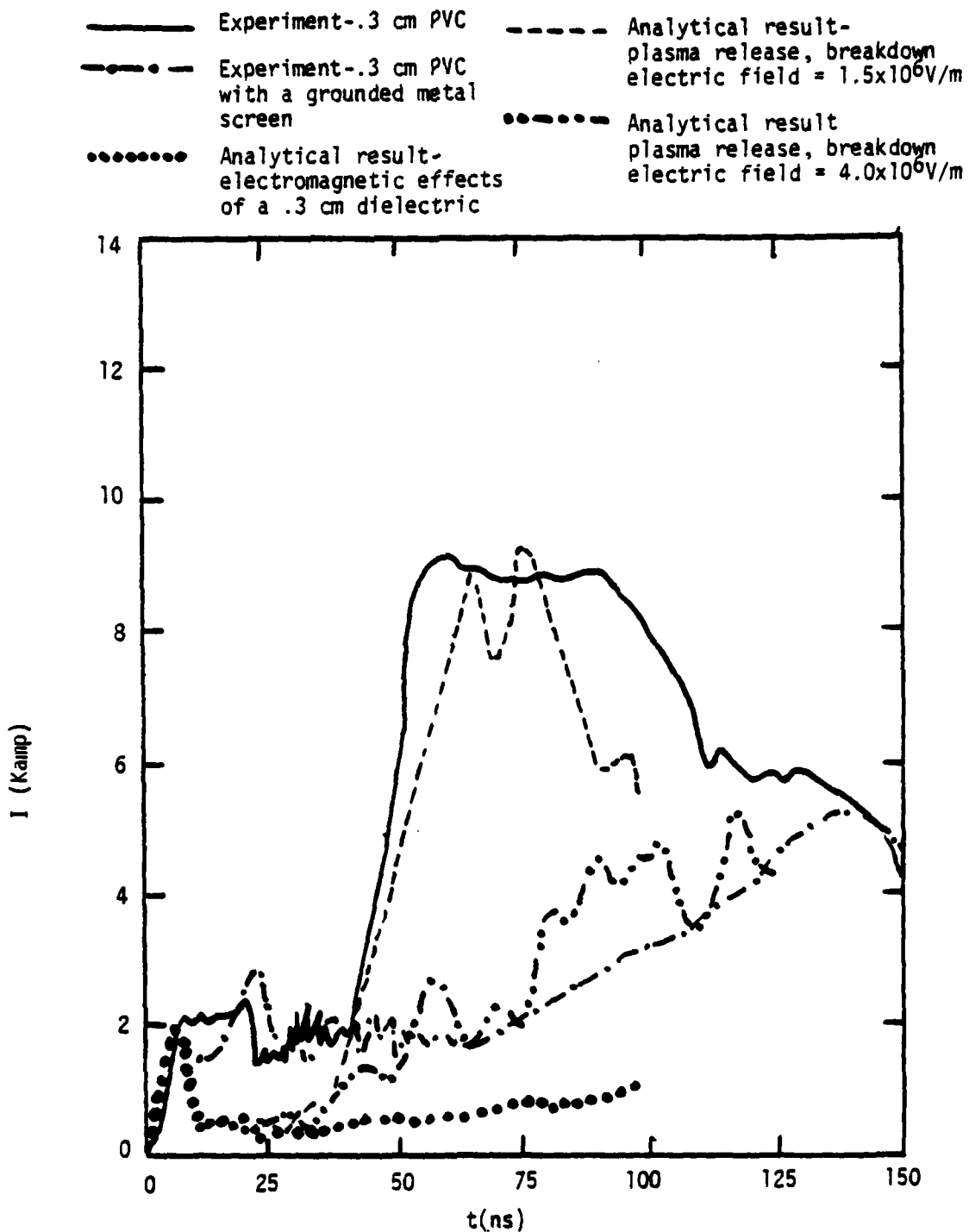
Figure 13

Empty Cavity Results

Figure 14

A Comparison Between Some Experimental and
Analytical Dielectric Results

V. CONCLUSION

While we have not identified the current enhancement process, we have eliminated dielectric charging as a possibility. We have demonstrated that an enhancement can be achieved with the emission of a neutral plasma from the dielectric surface. The resulting enhancement was found to be a function of the value of the threshold electric field.

In order to better understand the behavior of dielectrics, one would like to compare the present analytical model with experiments utilizing different geometries, electron beam energies fluences, etc. In addition, it would be useful to do more basic research, such as performing a plasma detection experiment.